

the centerline of the shock tube—some variation with vertical position was observed. Along with these data in Fig. 3 is a line representing the JPL thermochemical calculation of expected electron density. Generally, the present holographic measurements indicate an electron density 30% more than the calculation.

Spectroscopic Measurements of Electron Density

The path length across the diameter of the shock tube is quite long (15.3 cm) and reabsorption becomes appreciable for electron density of the order 10^{16} cm^{-3} or higher. The half-intensity width must be corrected for reabsorption; otherwise errors of 25% or more in the determination of the electron density may be incurred. The spectroscopic measurements reported here complement the previous effort described in Ref. 2 with the additional aspect that, besides covering new shock conditions simulating outer planet entry for a realistic hydrogen-helium composition, we take into account the influence of reabsorption on the line profile, which was neglected previously. Furthermore, our analysis is based on the improved Kepple-Griem⁵ treatment on Stark broadening instead of an earlier version by Griem et al.⁶ The measured electron density for 84.17% H_2 –15.83% He with initial pressure 1 torr from H_β profiles corrected for reabsorption are shown in Fig. 3, where measurements by holographic interferometry are also shown.

Conclusions

Experimental determination of the ionization relaxation distances and electron density has been made by means of holographic interferometry and spectroscopic measurements over a wide range of shock conditions (26–46 km/sec at an initial pressure of 1 torr) for a realistic composition (84.17% H_2 –15.83% He) simulating outer planet entry. As the shock velocity increases, the electron density increases while the relaxation distance decreases, as expected. There is good agreement between the results obtained from the holographic interferometry measurements and the spectroscopic measurements, which are two completely independent diagnostic techniques. In general, the equilibrium electron density determined from the experimental measurements is about 30% more than that predicted by the JPL thermochemistry code at shock speed from 26–33 km/sec. The extent of the nonequilibrium ionization zone measured with the holographic interferometer agrees qualitatively with H_α line emission measurements made by previous investigators at this laboratory over the shock speed range duplicated by each instrument. The range of test conditions covered by this work gives more realistic simulation of the entry conditions into Saturn nominal and Jupiter nominal atmospheres than previous experimental investigations.

References

- Leibowitz, L. P., "Attainment of Jupiter Entry Shock Velocities," *AIAA Journal*, Vol. 13, March 1975, pp. 403–405.
- Menard, W. A. and Stickford, G. H., "A Shock Tube Study of Thermal Radiation from Hydrogen-Helium Plasmas," Southeastern Seminar on Thermal Sciences, 10th Anniversary Meeting, April 1974, New Orleans, La., pp. 400–425.
- Leibowitz, L. P., Menard, W. A., and Stickford, Jr., G. H., "Radiative Relaxation Behind Strong Shock Waves in Hydrogen-Helium Mixtures," *Recent Development in Shock Tube Research, Proceeding of the Ninth International Shock Tube Symposium*, Stanford University Press, Stanford, Calif., 1973, pp. 306–317.
- Leibowitz, L. P. and Kuo, T. J., "Outer Planet Entry Nonequilibrium Heating," AIAA/AGU Conference on the Exploration of the Outer Planets, AIAA Paper 75-1149, 1975.
- Kepple, P. C., "Improved Stark-Profile Calculations for the First Four Members of the Hydrogen Lyman and Balmer Series," Dept. of Physics and Astronomy, University of Maryland, College Park, Md. Rept. 831, 1968, pp. 74–95.
- Griem, H. R., *Plasma Spectroscopy*, Chap. 4., McGraw-Hill, New York, 1964.

Analytical Comparison of the Performance of Different Base-Burning Modes

J. A. Schetz,* S. Favini,† and F. S. Billig‡
Applied Physics Laboratory,

The Johns Hopkins University, Silver Spring, Md.

Introduction

THE notion of "base burning" in an attempt to reduce the drag, or even provide thrust, on supersonic projectiles has been of interest for a number of years. In recent times, suggestions for locating the heat release zone adjacent to, but outside of, the viscous base flow have been presented² with a view toward improving performance. One also can envision combined systems where part of the energy is released in the base flow region and part to the outside. Unfortunately, there have been no direct experimental or analytical comparisons of these various schemes in terms of performance.

Earlier, we presented a simplified treatment of pure base-burning cases,² and it is the purpose of this Note to report on an extension of that work such that cases with all external burning or combined schemes can also be treated. Finally, a direct comparison of performance for a specific example is given.

Analysis

The original base-burning analysis² has been extended to include external burning processes using the flow model shown in Fig. 1. Transverse fuel injection is assumed to produce an oblique shock which turns the flow from the body axis to angle α . External burning turns it back to the horizontal, and α is proportional to $h_f f_s$, the product of the heating value of the fuel and its stoichiometric fuel-air ratio. It is assumed implicitly here that the injection process is tailored to $h_f f_s$ so as to produce a uniform, horizontal, but compressed flow external to the base region. This process then can be coupled to the base-burning analysis.

We may write the pressure change due to heat release as³

$$C_p = \frac{(\gamma - 1) q}{\rho_1 u_1 (\gamma R T_1) (M_1^2 - 1)^{1/2}} \frac{\sin \mu}{\sin (\mu + \alpha)} \quad (1)$$

where μ is the local Mach angle, γ the ratio of specific heats, ρ_1 , u_1 , T_1 , and M_1 are the density, velocity, temperature and Mach number behind the injection shock, respectively, and q is a heat rate per unit time and area, assumed uniform in space. This last assumption can be easily removed. It remains now to calculate the heat release that results from the combustion with air entrained into the fuel-rich external mixing zone. This entrainment rate can be estimated as for the base mixing region² noting that there are two sides to the mixing region here. Thus

$$dm/dx = 2k \rho_1 u_1 [1 - (\rho u / \rho_1 u_1)] = 2k \rho_1 u_1 \quad (2)$$

Received April 16, 1976. This work was supported by the Naval Ordnance Systems Command.

Index categories: Jets Wakes, and Viscid-Inviscid Flow Interactions; Airbreathing Propulsion, Subsonic and Supersonic; Combustion in Gases.

*Consultant; also Professor and Chairman, Aerospace and Ocean Engineering Department, Virginia Polytechnic Institute and State University.

†Senior Programmer.

‡Supervisor, Submarine Physics.

Table 1 Comparison of base pressure rises

Configuration	$\dot{m}_{\text{fuel}}/\rho_1 u_1 h$			p_b/p_∞	p_1/p_∞	ℓ/h	f_s	$(T_0)_{\text{throat}}$	M_j
	Total	Base	Side						
All base	0.213	0.213	...	1.08	1.00	69	0.383	2220	0.688
	0.162	0.162	...	1.05	1.00	78	0.256	2300	0.527
	0.050	0.050	...	0.87	1.00	73	0.81	2500	0.212
Combined base/EB	0.213	0.062	0.151	1.08	1.21	105	0.073	2500	0.227
All EB	0.023	...	0.023	0.51	1.21	16	0.073

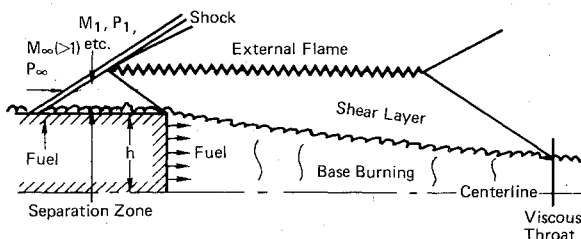


Fig. 1 Schematic of flowfield model with external burning.

with $k=0.01$. Again following our work for the base region, the entrained air has an effective heating value when combined with the fluid in the fuel-rich zone, so that

$$q = c_p \dot{m} dT_0 = d\dot{m} [h_f f_s + c_p (T_{01} - T_0)] \quad (3)$$

If the first term in the brackets is much larger than the second, or if both terms are contained into an "effective" heating value $(h_f f_s)_{\text{eff}}$, then

$$q = \dot{m}_{\text{air}} (h_f f_s)_{\text{eff}} / \ell \quad (4)$$

where ℓ is the length of the flame. Finally

$$C_p = \frac{(\gamma - 1) 2k (h_f f_s)_{\text{eff}}}{(\gamma R T_1) (M_1^2 - 1)^{1/2}} \frac{\sin \mu}{\sin(\mu + \alpha)} \quad (5)$$

The minimum amount of fuel required to produce this situation can be back-calculated as follows. First, ℓ is found from the base-flow analysis such that the last wave from the external burning region strikes the base flow at the viscous throat. The air contained in this length equals

$$\dot{m}_{\text{air}} = 2(k) \rho_1 u_1 \ell \quad (6)$$

so that the fuel required is

$$\dot{m}_{\text{fuel}}/\rho_1 u_1 h = \dot{m}_{\text{air}} f_s/\rho_1 u_1 h = 2k f_s (\ell/h) \quad (7)$$

Results

Consider now a specific situation

$$M_\infty = 2.3; T_{0\infty} = T_{01} = 1000^\circ R; \gamma = 1.4$$

$$(T_0)_{\text{fuel}} = 1150^\circ R; (\delta/h) < 0.1;$$

$$\text{and } (h_f f_s/C_p)_{\text{eff}} = 1600^\circ R$$

with three different configurations: all base-burning, all external-burning (EB), and combined EB/base-burning. In Table 1, compare the first entry in the all-base situation with the combined EB-base case. They have the same total fuel flow and virtually the same base pressure level. The high EB fuel flow rate for the combined case is a direct result of the very long base flow region ($\ell/h = 105$) predicted with substantial heat release and a low base injection rate. The fuel/air ratio f_s is obtained with the assertion that all of the fuel in-

jected through the base is consumed by the viscous throat. Put another way, the mixture is fuel-rich or at least stoichiometric up until the viscous throat.

The results for the all-EB case are particularly informative: the base region is short ($\ell/h = 16$), so that the required fuel flow [see Eq. (7)] and resultant p_b/p_∞ are low. Increasing the fuel flow rate for this case beyond the level shown will not increase p_b , since air will not be available for combustion until beyond the point where EB can effect the base flow ahead of the viscous throat and change p_b . Higher p_b might be achieved, however, by stacking (or staggering injectors with the initial compression wave of each flame sheet intersecting the corner of the base), increasing the air entrainment rate, and assuming discrete-hole injection instead of an injection sheet.

References

- ¹Strahle, W. C., "Theoretical Considerations of Combustion Effects on Base Pressure in Supersonic Flight," *Twelfth International Symposium on Combustion*, 1968 Poitiers, France.
- ²Schetz, J. A., Billig, F. S., and Favin, S., "Simplified Analysis of Supersonic Base Flows Including Injection and Combustion," *AIAA Journal*, Vol. 14, Jan. 1976, pp. 7-8.
- ³Tsien, H. S. and Beilock, M., "Heat Source in a Uniform Flow," *Journal of Aeronautical Science*, Dec. 1949, p. 756.

Pit Formation on the Accelerated Solid Propellant Combustion Surface

Tohru Mitani*

National Aerospace Laboratory, Miyagi, Japan

Introduction

IT has been reported that the burning rate of solid propellants increases in the acceleration field. This phenomenon is caused by the local burning rate increases (pit formation) by agglomerated aluminum spheres on the accelerated combustion surface. Many experimental and analytical studies have been carried out regarding this acceleration-induced burning rate increase of solid propellants. But all of the studies are concerned with the mechanism of local heat feedback on each pit, not with the density or distribution of pits themselves. Up to the present time, no detailed investigation except a paper by Niioka, et al.¹ has been published concerning the pitting phenomenon on the accelerated combustion surface. In order to clarify the acceleration sensitivity of solid propellants, however, it is necessary to study the pitting mechanism. This is because the pitting mechanism determines the transient period of combustion^{2,3} the instantaneous

Received April 19, 1976; revision received May 19, 1976.

Index categories: Combustion in Heterogeneous Media; Fuels and Propellants, Properties of.

*Research Engineer, Kakuda Branch.